THE FEASIBILTY OF PXRF FOR DISCRIMINATING ATTIC BLACK-FIGURE PAINTERS USING PIGMENT ANALYSIS

Üftade Muşkara[1] and Kübranur Kalaycı[2]

[1]*Kocaeli University, Faculty of Fine Arts, Department of Conservation and Restoration of Cultural Properties, Turkey*
[2]*Kocaeli University, Institute of Social Sciences, Department of Archaeology, Turkey*

ABSTRACT

To investigate the possibilities of identifying Attic vase painters based on element compositions, ten black-figure vases preserved in the Izmir Archaeological Museum were analyzed using a handheld XRF, Hitachi instrument. This technique enables in situ analysis of the museum objects and surface analysis of whole vases. Vases attributed to Gorgon Painter, Sophilos, KY Painter, Rhodos 12264 Painter, Lydos, Affecter, Antimedes, and Leagros Group were selected as the study group. Higher Zn levels in the black gloss, dark red, and white paint areas than the corresponding ceramic bodies were detected. Elevated V and Cu levels were also determined in black gloss and dark red layers. When Zn/Ti ratios in the body, dark red paint, and black gloss are plotted, vases by Sophilos and Lydos show similar compositional signatures. Therefore, we argue that the chemical composition of the paints could reveal painters' characteristics based on the hypothesis that dark red and white paints could have been prepared by painters as a special mixture of their own.

1. INTRODUCTION

1.1. *Attic Black-Figure Vase Painters*

Although the technique was first invented by Corinthian vase painters, it was adopted by Attic painters, and Athenian black-figure pottery production took over the Mediterranean market by the middle of the 6th century (Boegehold, 1985). The attribution of these vases to individual hands based on close examination of the artistic style is essential because it makes it possible to date the vases within a short period. Sir John Beazley certainly played a significant role in the attribution of tens of thousands of Athenian painted vases to artists, schools, and manners (Morris, 1994).

Achilles was the first painter as an artist identified by Beazley. Following this, many vase painters were recognized based on their signatures or/and styles. However, we do not have any historical document on the artists who made and paint the vases, which explains their names, age, sex, and how they produced them (Turner, 2000). Furthermore, there are many questions regarding the real meaning of the signatures "epoiesen" (made) and "egraphsen" (wrote) (Cohen, 1991; Liassarrague, 1997; Pevnick, 2010). Attic vases were distributed around the Mediterranean and the Black Sea region through trade. Therefore, Beazley's elaborate list of painters and the chronology based on the stylistic development of painters are useful tools for an archaeologist who wishes to establish a chronology for a specific site. Meantime, the well-documented Attic black-figure pottery provides information on exchange systems and cultural relations as well.

1.2. *Archaeometric Analysis of Painted Layers of Attic Pottery*

The black-figure technique of vase painting involves drawing figures and motives in silhouette on the leather-hard surfaces using slip material. Incisions were applied for elaborated details, while vase painters also used dark red-purple and white colors for further minutiae. To achieve the desired shiny metallic black color for the slip, ancient potters employed single firing involving three stages of the oxidizing, reducing, and oxidizing (ORO) conditions. Many studies on the quality of black gloss and the determination of firing techniques of Attic pottery showed that at a maximum firing temperature of 890-950°C, iron-rich clays turned black (magnetite Fe_3O_4, wustite FeO or hercynite $FeAl_2O_4$) and vitrified during the reducing stage of firing (Gangas et al., 1976; Tite et al., 1982; Maniatis et al., 1993; Lühl et al., 2014).

Previous studies suggested that the black slip material was indeed the refined clay produced by flocculation of the same clay used for the body of the pots. However, developing technologies provided non-destructive analysis for further investigation to understand the micromorphology and element composition of the black gloss. Such studies demonstrated that the composition of the black gloss was sufficiently different to consider using a clay source special for the slip material and application of a standard procedure for refining the clay (Kingery, 1991; Maniatis et al., 1993; Tang et al., 2001; Aloupi-Siotis, 2008; Chaviara and Aloupi-Siotis, 2016. Aloupi-Siotis (2020) recently suggested that the ancient potters should have selected the raw material for the slip, which should be rich in illite minerals and low in $CaCO_3$ to obtain the desired final product. She showed that the quality of black gloss depend on some parameters such as the slip material (or mixture), the application method, and the ORO firing scheme. She also proposed the term "Black glass-ceramic or Fe-BGc" to describe iron-based coating instead of black gloss because the characterization studies revealed its ceramic-glass nature. Walton et al. (2015), on the other hand, investigated the refinement methods for the slip material (2015). They found higher Zn concentrations on the corresponding black gloss layer and proposed that the acid-containing zinc in the form of vitriol might have been added to the body clay during the preparation of slip material to induce flocculation to remove the remaining $CaCO_3$. However, Chaviara and Aloupi-Siotis (2016) argued that vitriol treatment would cause low pH of the aqueous solution that would lead to coagulation of clay platelets, and the acidic slip material destroyed the body during the application in the experimental productions. Consequently, the sophisticated firing procedures and the preparation method of black gloss suggest technological knowledge and specialized labor in the pottery manufacture for the black-figured vases.

Meantime, the number of analytical studies on the characterization of the added colors, red-purple or white, of black-figure pottery is still limited. Mitri et al. (2006) made significant contributions to the pigment analysis of Attic red-purple and white paints, while Mastrotheodoros et al. (2010; 2013) worked on the vases produced in other workshops and the production of ancient pigments. In this work, the term "dark red" was accepted for the added red color applied for decorations.

The research on the black figure amphora attributed to Priam Group by Mitri et al. (2006) proposed that due to the higher iron concentration (55 wt%), dark red was probably prepared as mixing an iron ochre with a refined low-calcareous clay, which

was selected with similar characteristics to the clay decided for the black gloss (2006). The unusual dark red color (as different from the background red) was due to the partial re-oxidation of FeO, and the combination of FeO and Fe_2O_3 lead to the dark red color. For the purple color used on the decorations of Corinthian and Theban pottery, Mastrotheodoros et al. (2010; 2013) also agreed that a mixture of clay and an iron-rich raw material could have been used due to the higher Fe concentration (30–47 wt% Fe_2O_3); however, another crucial reason for the purple hue was the particle size of hematite with diameters above 0.4 mm which was formed at a temperature around 900°C. The results imply that the preparation of the pigment mixture should have been controlled by the painters since the amount and the particle size of the iron ochre are highly influential on the color's final hue.

For the white paint layers on the group of pottery from different workshops, including Theban, Corinthian, Euboean, Mastrotheodoros et al. (2013) observed that the white paint was applied prior to the firing, and there were considerable differences regarding the thickness of the white pigments, although they exhibited similar morphological features. According to the low Al_2O_3/SiO_2 ratio, white paint layers were found to be made of coarser raw material. Ca or Mg clays were used as a white pigment; however, Cao/MgO ratios of different vases did not indicate a correlation with specific workshops.

Examining the chemical composition of paints used in the decorations in detail could expand our understanding of the operational sequence, chaîne opératoire, all the stages of ceramic manufacture from raw material to the final product (Roux, 2020), and the role of painters in the pottery industry at Attica. This study aims to investigate the chemical composition of the body, black gloss, dark red and white paints of Attic black-figure vases preserved in İzmir Archaeology Museum to identify compositional groups that characterize individual painters. The data presented here is an initial work to recognize whether it is possible to discriminate the vase painters or ateliers based on the element distribution of paints.

We design the research question of the study as
- Is it possible to verify the accuracy of attribution studies with analytical techniques?

We set hypotheses of the study as
- Added red and white paints should be prepared by painters as a unique mixture of their own,
- The chemical composition of added red and white paints would reveal painters' characteristic palette,
- Using a handheld XRF instrument would indicate the differences in elemental compositions of the paints.

2. MATERIALS AND METHODS

2.1. Archaeological Samples

In Table 1, the vases in İzmir Museum that were selected for the study are listed. Some of the vases were studied by archaeologists and attributed to specific black-figure vase painters. Among the ten vases, two of them were attributed to Sophilos, one to Gorgon Painter, Rhodos 12264 Painter, and KY Painter. Two oinochoe could be attributed to Lydos, the belly amphora to Affecter, and the lekythos to Antimenes Painter. Ten vases represent the early and the later black-figure periods. Further details on the decorations of the vases are given in the catalogue (Appendix 1).

Table 1. Study Group of Black-Figure Vases From İzmir Archaeological Museum

Inventory Number	Sample Number	Form	Painter	Date	Image	Detail Images
005.811	GP	Olpe	Gorgon	600-575 BC		

003.332	SP1	Lebes Gamikos	Sophilos	580 BC		
009.537	SP2	Louterion	Sophilos	580-570 BC		
005.662	KYP	Kylix	KY	575-565 BC		
013.753	RP	Siana Kylix	Rhodos 12264	540 BC		
008.089	LP1	Oinochoe	Lydos	540 BC		

004.889	LP2	Oinochoe	Lydos	560-550 BC		
008.090	LGP	Lekythos	Leagros Group	550-500 BC		
012.456	AP	Amphora	Affecter	550-500 BC		
016.582	ANP	Lekythos	An-timenes	550-500 BC		

2.2. Analytical Methods

The macro-morphological investigation was done with Nikon D610 using natural side lighting under the same conditions. Surface analysis of the vases was conducted with a handheld XRF, Hitachi X-Met8000 Expert specialized for archaeometric studies. Although there are certain analytical limitations of pXRF, it has been an increasing application, especially for in-situ, non-destructive, surface analysis and painted layers (Cesareo et al., 2008; Williams-Thorpe, 2008; Shackley 2011; Liritzis and Zacharias, 2010; Kaplan et al., 2014; Liritzis et al., 2018, 2020; Ali et al., 2020). Even when the instrument is calibrated with reference materials, the result should be evaluated with caution

due to the nature of the technique, the matrix of the material, surface geometry, and thickness. The penetration depth, fluorescent X-rays' capability to escape from the sample's matrix, and the surface thickness make the analysis highly complicated for painted layers. Nevertheless, the semi-quantitative or qualitative analysis could provide valua-ble information on the manufacturing technologies. In the study by Foster et al. (2011), the authors tested the impact of some parameters, including surface morphology, grain size, and mineralogy, on the pXRF analysis of heterogonous handmade pottery. They demonstrated that with appropriate methodologies such as element choices, a sufficient number of replicates, and a homogenous matrix, it is possible to identify different compositional groups with pXRF analysis. We know successful application of pXRF on various types of ware including Attic black-figure, Cypro-Geometric, Cypro-Archaic Bichrome, Mycenaean, and White Mountain Red Ware in east-central Arizona.

To identify the paint "recipes" of Ancestral Pueblo pottery from the US Southwest, Duwe and Neff (2007) proposed a methodology, including PCA and bivariate plots of the element data determined by time of flight-laser ablation-inductively coupled plasma-mass spectrometry (TOF-LA-ICP-MS). Van Keuren et al. (2013) later investigated the time scale and geological distributions of specific recipes. Ferguson et al. (2015) expanded this study by applying pXRF to whole vessel decoration. They examined the qualitative composition of painted decorations on White Mountain Red Ware to understand any possible correlation between the compositional group of paints and decoration schemes on the vases. When the data were compared to the analysis by LA-ICP-MS, the results showed that pXRF were capable of identifying previous groups as well. They were also able to detect that multiple paint mixtures were applied on a single vessel to achieve different hues. Most recently, in the study of the characterization and the provenance of a group of Mycenaean pottery sherds, Liritzis et al. (2020) mentioned some of the trace elements determined by pXRF, particularly V and Cr, exhibited considerable variability across the surface of the same sample probably due to sample geometry and the surface porosity. Therefore, these elements were not selected for multivariate analysis, including principal component analysis (PCA) and hierarchical cluster analysis.

In this study, the apparatus was equipped with a silicon-drift detector (SDD) and excitation source of X-ray tube Rh target. For the analysis of high-energy and lower mass trace elements (V, Cr, Mn, Co, Ni, Cu, Zn, As) and some major elements (Ca, Fe, and Ti), the instrument was set to 40 kV for 120 s. The software provided by Hitachi was adjusted to Compton normalization for the analysis. The analysis spot size was 3 mm, and an integrated camera was included for accurate positioning of the analyser. The elements suggested in the literature were selected for analysis to control the penetration depth of radiation through the layers (Shoval and Gilboa, 2015; Chaviara and Aloupi-Siotis, 2016; Aloupi-Siotis, 2020). In order to confirm the analyser accuracy and stability, secondary standards were used before and during the analysis.

Moreover, since the thickness of the layers was important for XRF studies, visual observations of painted layers by digital photography were applied before the analysis. The examination of photo-macrographs revealed the most appropriate location of the layer where the pigments were best preserved. The measure-ments were then applied at least five times for each paint layer along with the clay paste. For dark red and black painted areas, the measurements with the highest Zn content and the white-painted areas the measurements with the highest Ca content were selected. Moreover, the results were also compared with the published values elsewhere, although different analytical methods were applied (Aloupi-Siotis, 2020)

3. RESULTS AND DISCUSSION

The mean concentrations of major elements (wt%) and trace elements (µg/g) of body, dark red, black gloss, and white layers of vases on a semi-quantitative basis are presented in Tables 2-5. Compositional groups were identified by PCA using the data (TiO, CaO, Cr, Ni, Cu, Zn, As) for body clay pastes and painted layers for each vase (Buxeda i Garrigós et al., 2003; Duwe and Neff, 2007; Van Keuren et al., 2013; Ferguson et al., 2015). PCA was performed using a correlation matrix with no rotation axis. Base-10 log-transformed data were used for the concentrations.

Table 2. PXRF analyses of the ceramic body of the vases (the results are the mean of n=5, n.d. not detected)

Body (n=5)	GP	SP1	SP2	KYP	RP	LP1	LP2	LGP	AP	ANP
Fe_2O_3 (wt/%)	8.02±0.20	9.01±0.32	8.85±0.35	9.65±0.31	9.30±0.37	8.90±0.29	8.96±0.29	9.34±0.32	8.90±0.30	8.78±0.27
CaO (wt/%)	6.43±0.47	7.89±0.64	10.52±0.78	4.20±0.97	3.03±0.25	7.26±0.57	4.24±0.85	6.34±0.43	5.86±0.26	4.40±0.39
$TiO2$ (wt/%)	0.95±0.02	0.69±0.01	0.70±0.08	0.97±0.04	0.65±0.05	0.76±0.04	0.66±0.05	0.81±0.07	0.75±0.02	0.94±0.07
V ($\mu g.g^{-1}$)	102±5	85±5	57±5	76±9	117±9	55±4	87±6	104±5	95±2	59±3
Cr ($\mu g.g^{-1}$)	404±7	321±3	310±4	421.5±7	347±3	340±3	322±2	352±4	386±8	338±3
Mn ($\mu g.g^{-1}$)	871±18	637±18	742±19	760.5±16	749±15	779±18	850±21	732±18	767±10	870±15
Co ($\mu g.g^{-1}$)	71±5	82±5	65±5	45±4	n.d.*	50±4	n.d.	64±5	n.d.	87±4
Ni ($\mu g.g^{-1}$)	340±5	363±6	353±6	411±19	329±5	365±6	303±9	371±6	407±9	308±11
Cu ($\mu g.g^{-1}$)	70±3	66±3	75±3	73±7	50±3	84±3	61±4	113±4	71±3	54±2
Zn ($\mu g.g^{-1}$)	152±2	227±3	229±3	222±12	141±2	173±7	207±13	174±3	162±5	174±3
As ($\mu g.g^{-1}$)	24±1	30±1	32±3	22±4	44±1	24±2	13±1	40±2	33±4	73±3

Table3. PXRF analyses of the black gloss layers of the vases (the results are the mean of n=3)

Black Gloss (n=3)	GP	SP1	SP2	KYP	RP	LP1	LP2	LGP	AP	ANP
Fe_2O_3 (wt/%)	9.01	9.94±0.32	10.86±0.31	11.68±0.13	11.05±0.20	12.23±0.13	10.57±0.36	10.23±0.49	9.51±0.37	10.78±0.46
CaO (wt/%)	1.60±0.01	1.48±0.01	2.77±0.02	1.72±0.37	3.05±0.22	1.76±0.07	3.32±0.03	2.45±0.06	1.58±0.05	1.16±0.07
$TiO2$ (wt/%)	0.45±0.01	0.48±0.01	0.52±0.01	0.55±0.04	0.75±0.02	0.55±0.03	0.62±0.02	0.57±0.01	0.42±0.03	0.57±0.04
V ($\mu g.g^{-1}$)	132±7	136±3	134±10	144±11	138±4	130±2	112±3	116±3	118±4	163±14
Cr ($\mu g.g^{-1}$)	304±5	323±6	347±6	349±12	371±3	350±7	248±11	335±5	320±5	298±11
Mn ($\mu g.g^{-1}$)	625±17	594±20	766±22	721±13	851±19	835±18	896±14	587±13	613±16	822±23
Co ($\mu g.g^{-1}$)	n.d.	39±2	46±1	34±4	n.d.	41±2	n.d.	52±2	n.d.	n.d.
Ni ($\mu g.g^{-1}$)	254±3	313±5	357±8	371±12	380±7	383±3	236±9	333±6	317±4	294±7
Cu ($\mu g.g^{-1}$)	39±2	42±4	88±9	48±6	40±3	60±5	38±1	85±7	45±2	44±2
Zn ($\mu g.g^{-1}$)	416±20	373±13	387±15	437±18	191±15	238±17	240±10	284±12	544±25	501±27
As ($\mu g.g^{-1}$)	32±1	33±1	53±7	29±3	47±3	43±2	19±1	34±1	42±1	86±2

Table 4. PXRF analyses of the dark red paints of the vases (the results are the mean of n=3)

Dark Red Paint (n=3)	GP	SP1	SP2	KYP	RP	LP1	LP2	LGP	AP	ANP
CaO (wt/%)	4.79±0.65	2.13±0.51	3.27±0.48	1.73±0.25	3.67±0.27	3.22±0.31	3.52±0.24	5.14±0.81	3.61±0.12	1.10±0.41
$TiO2$ (wt/%)	0.61±0.05	0.41±0.02	0.48±0.04	0.58±0.01	0.68±0.03	0.52±0.03	0.72±0.02	0.70±0.01	0.43±0.01	0.34±0.03
V ($\mu g.g^{-1}$)	80±4	96±10	78±7	108±12	108±11	109±8	61±7	68±12	73±4	108±7
Cr ($\mu g.g^{-1}$)	333±5	250±8	217±3	349±8	337±4	302±7	276±5	311±7	319±3	237±4
Mn ($\mu g.g^{-1}$)	1288±22	727±16	537±14	1078±29	824±17	562±18	819±23	678±28	693±24	1197±19
Co ($\mu g.g^{-1}$)	n.d.	n.d.	n.d.	n.d.	n.d.	36±3	n.d.	n.d.	n.d.	n.d.

Ni (µg.g⁻¹)	338±7	271±9	243±5	319±1	347±3	295±4	234±6	345±8	350±1	268±5
Cu (µg.g⁻¹)	59±2	87±4	118±7	127±7	74±4	76±5	78±5	120±8	117±10	102±7
Zn (µg.g⁻¹)	164±7	338±12	422±15	381±16	213±9	175±6	306±9	350±21	473±15	441±19
As (µg.g⁻¹)	30±2	58±4	59±1	37±6	106±5	64±2	43±2	42±3	51±4	170±12

Table 5. PXRF analyses of the white paints of the vases (the results are the mean of n=3)

White Paint (n=3)	SP1	RP	LP2	LGP	AP	ANP
CaO (wt/%)	9.91±0.29	8.05±0.30	9.97±0.23	6.93±0.11	7.99±0.37	4.27±0.12
TiO2 (wt/%)	0.58±0.02	0.70±0.01	0.58±0.05	0.63±0.01	0.62±0.04	0.47±0.03
V (µg.g⁻¹)	106±11	70±7	73±9	103±7	85±13	60±3
Cr (µg.g⁻¹)	285±16	258±21	242±14	313±4	297±28	176±11
Mn (µg.g⁻¹)	599±21	882±19	1112±19	733±18	727±22	1027±15
Co (µg.g⁻¹)	74±2	76±2	99±7	39±3	70±5	65±2
Ni (µg.g⁻¹)	325±13	328±18	235±13	352±18	332±19	194±8
Cu (µg.g⁻¹)	60±9	63±10	58±6	88±7	53±5	50±4
Zn (µg.g⁻¹)	185±14	186±17	346±14	411±9	451±27	418±15
As (µg.g⁻¹)	46±3	71±8	34±4	45±9	40±3	79±4

3.1. Body

Figure 1 presents the body clay data classification by PCA and elemental variables for principal components 1 and 2. The concentrations of Fe_2O_3 of the body are found similar for all the vases (Table 2). However, CaO contents are different, the lowest for the kylix by RP and the highest for the louterion by SP1. This difference could be considered natural with respect to the size of the vases. It is known that the mechanical and thermal properties of vases, even for fine wares, can be modified using additives such as calcite (Maniatis et al., 2009). TiO_2 contents are also similar, which range between 0.65 and 0.97 wt%. V and As exhibit variability between the vases. The reason for V variation in the clay paste of the body could be due to surface irregularity, as explained by Liritzis et al. (2020). Although there is no obvious group separation is detected, interestingly, LP2 is distinguished from the remaining by its lower TiO_2 and Cr contents.
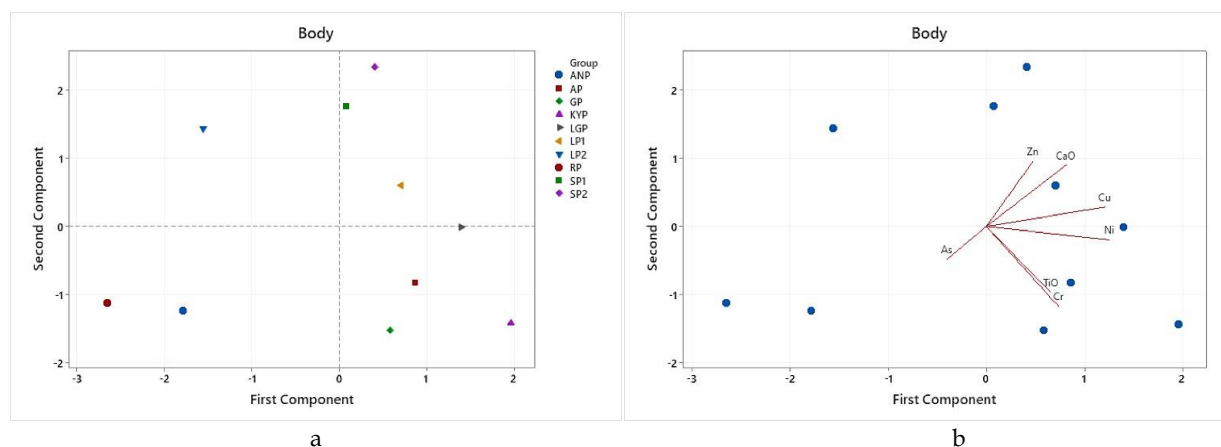

Figure 1. Bivarite plot of PCA using (a) body data and (b) score and loading plot for principal components 1 and 2.

3.2. Black Gloss

For the black gloss, Fe_2O_3 concentrations are relatively higher than the body (Table 3). The CaO contents of the vases are generally lower in black gloss than the body, as expected. The average concentration of Ca in black gloss was estimated around 1% for Archaic pottery (Aloupi and Maniatis, 1990; Maniatis et al., 1993; Maniatis et al., 2009). TiO_2 contents of black gloss layers are also found to be lower than the body except for RP. Previous studies mentioned elevated levels of Zn in black gloss, which could be related to the special preparation process or using a different clay source for the slip material (Walton et al., 2015; Chaviara and Aloupi-Siotis, 2016). In this study, the same situation is observed except for the vases LP2 and RP. Meantime, an enrichment of V is also calculated for the black gloss layers (Table 3). The elevated V concentrations in the black pigments were likewise found in a study on pigments in the decorations on the Cypro-Geometric and Cypro-Archaic ceramics

(Shoval and Gilboa, 2015). On the other hand, the variation observed on the body is not detected for the gloss layer; V concentration is between 112-163 µg/g. Figure 2 shows PCA applied for the data set from the black gloss. The black gloss layer of LP2 seems to be distant from the remaining as its body clay (Fig. 5a). No clear distinction between the black gloss layers could represent the clay mixture for the slip was prepared according to a straightforward process.
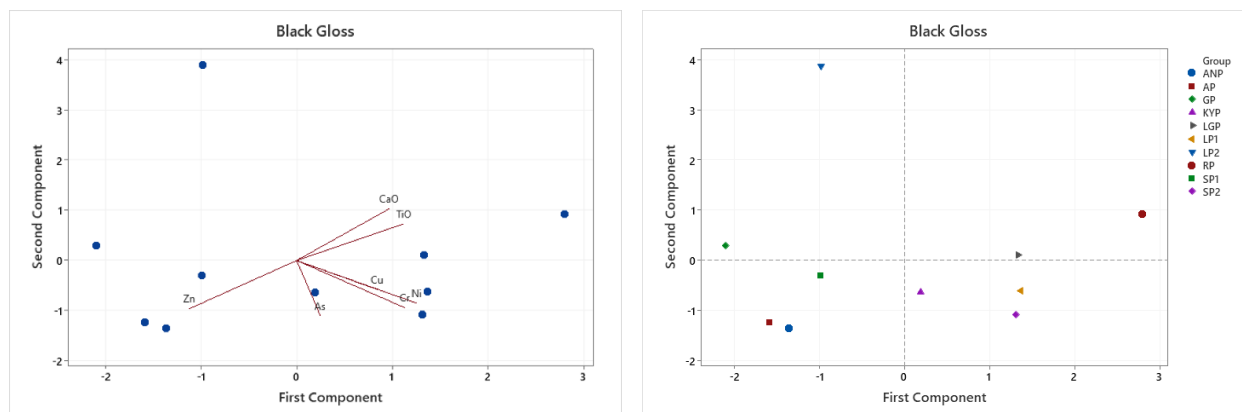

Figure 2. Bivarite plot of PCA using (a) black gloss data and (b) score and loading plot for principal components 1 and 2.

3.3. Dark Red Paint

An increase in the iron concentrations characterizes the dark red areas compared to the corresponding ceramic bodies and the black gloss layers. However, since the instrument calibration was adjusted to lower concentrations and the focus of the study is on the trace element compositions, the Fe_2O_3 concentrations are accepted as found in other studies around 30–55 wt% (Mastrotheodoros et al., 2013; Mitri et al.,

2006). As assumed, concentrations of CaO are lower than the body, however, higher than the black gloss. TiO_2 contents are similar to the corresponding black gloss layers. The high LOD of cobalt is due to the strong interference with iron since, in the dark red layers, the concentration Fe_2O_3 is larger than the concentrations in the ceramic body and black gloss. The Mn content varies between the vases, and the highest Mn concentrations are found in dark red layers of GP and KYP (Table 4).
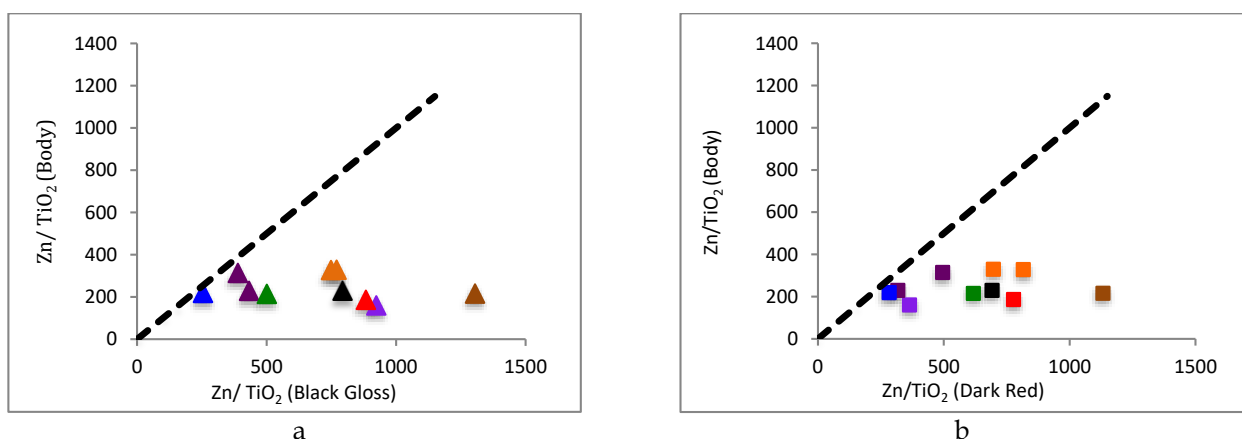
Figure 3. Enrichment diagrams of the 10 vases showing Zn fraction in the body versus for the black gloss (a) and the dark red layer (b) (Color code ■■■■■■-SP, GP, KY, LP, RP, AP, ANP, LGP).

Surprisingly, elevated Zn levels are also observed for dark red layers of the vases as for the black glosses. The enrichment-depletion plots of Zn are shown in Figure 3 (Walton et al., 2009). In the case of vases LP2 and RP, CaO and Zn concentrations are similar in black gloss layers compared to the ceramic bodies (Fig. 6). The coarser morphology and the reddish hue

on the black glosses of these vases can be observed in Figure 4. The effects of calcareous clay on the final color were explained by Maniatis et al. (2009), and the elevated levels of CaO + MgO in coral red slips were investigated by Walton et al. (2009). Nevertheless, the larger CaO measurements could be due to the thick-

ness of the layer and accordingly due to the contribution from the body during the analysis or to heterogonous distribution of Ca (Foster et al. 2011). The elevated Cu levels are also determined for dark red layers for some of the vases.

Figure 5 plots the scores and the loadings on the dark layers of vases on the first two principal components. Although the number of vases is limited, three major compositional groups appeared on the first two components (Fig. 4). One group (3 vases) is defined by high amounts of As, another one (4 vases) is marked by the lower amount of Zn and Cu. On the other hand, the third group (3 vases) is high in Zn and Cu. The large positive loading for Zn and Cu in the PC2 has seem to be in accordance with the data provided by Shoval and Gilboa (2015) for the red paints.

They described the larger concentrations of Cu and Zn in red paint pigments that were considered as associated with "red ferruginous pigment ore." A study by Popelka-Filcoff et al. (2007) was on the determination of variation in the element patterns of ochre from iron oxide sources to understand the differences better. Their results provided the information that using a combination of the Pearson's two-tailed correlation test and multivariate statistics for characterizing ochre were discriminative for the pigments. Elements that were found significantly positively correlated with Fe included V and Cu, although they indicated that these elements might not be universal for other sources. Moreover, they employed neutron activation analysis (NAA) on homogenous samples.

Figure 4. Details of the vases RP (a) and LP2 (b) for the black gloss and details of red paints of KYP and GP on the komast figure (c) and the lion (d).
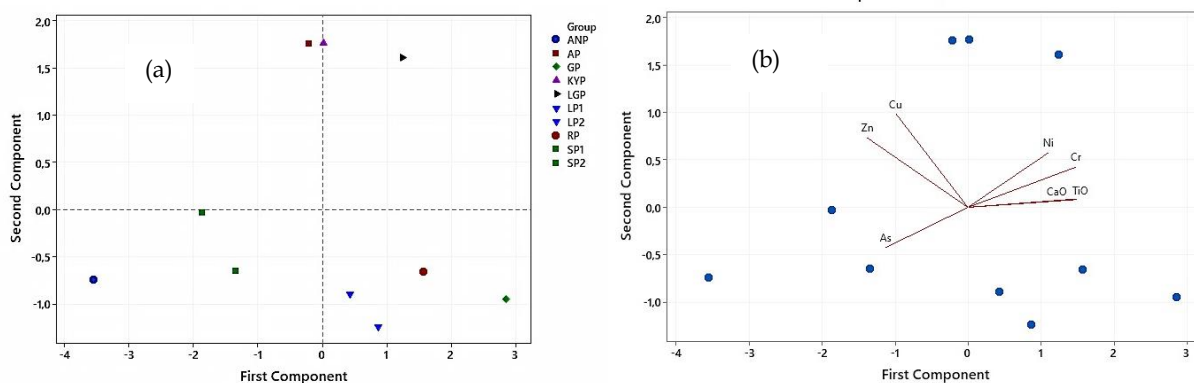
Figure 5. Bivariate plot of PCA using (a) red paint data with each case marked with same symbol if it was made by the same painter and (b) score and loading principal components 1 and 2.
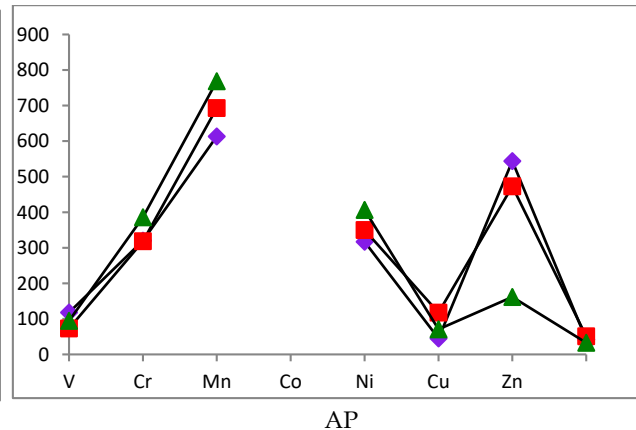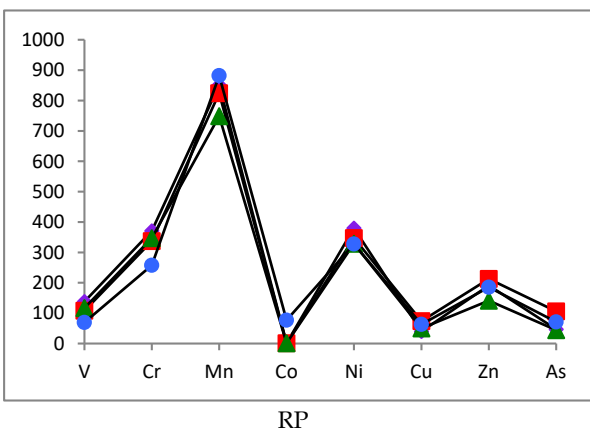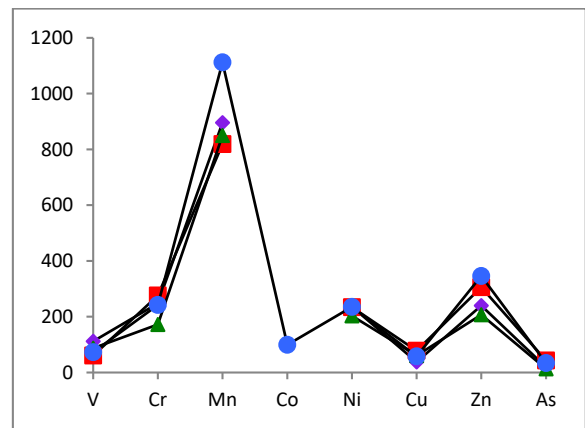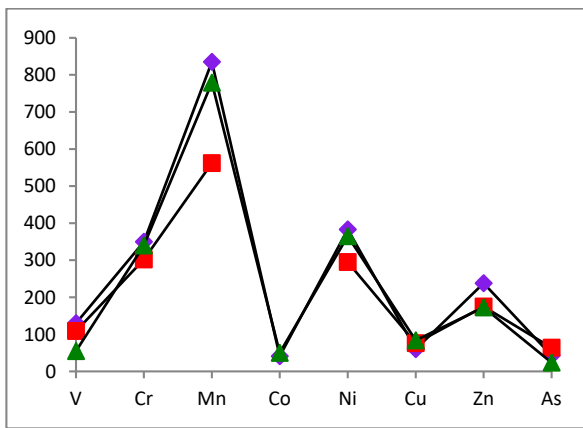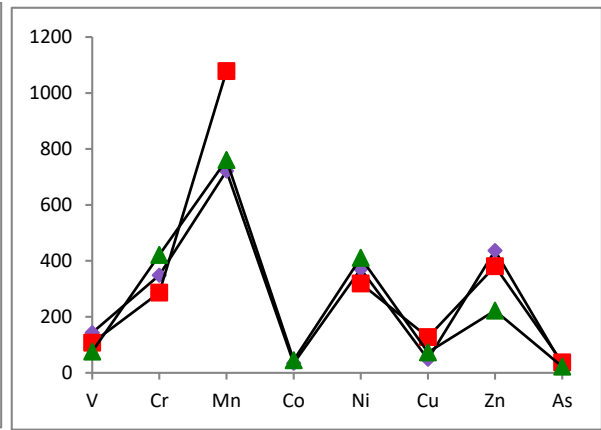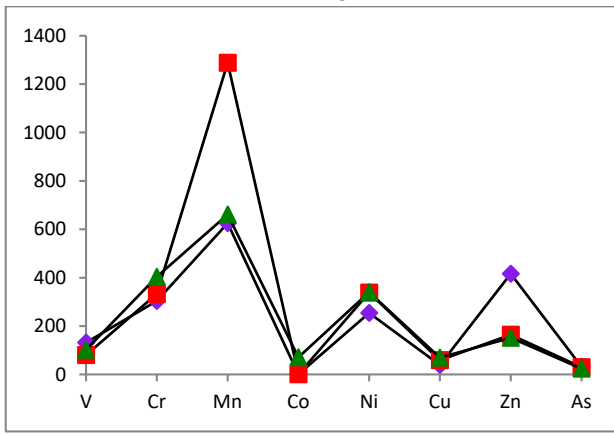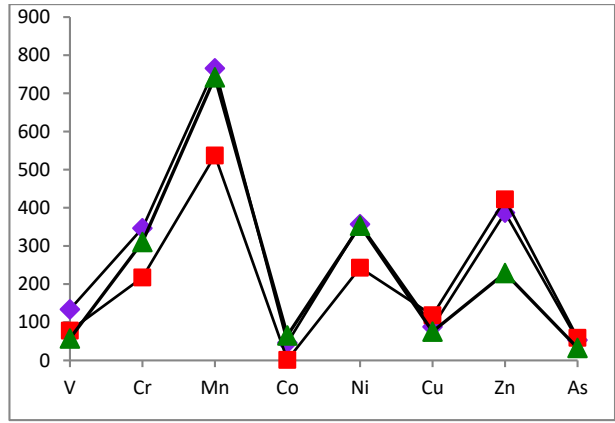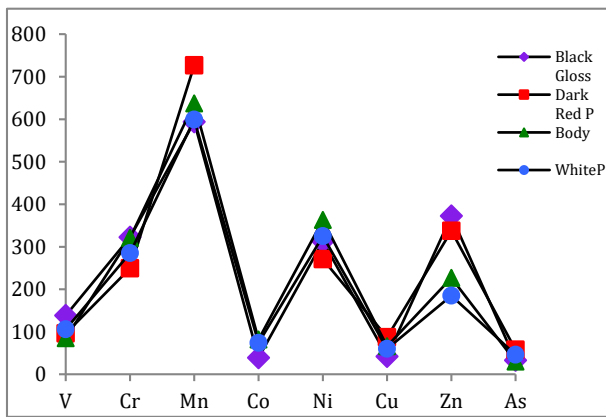
3.4. White Paint

White paint layers are found on the decorations of the vases SP1, RP, LP2, AP, LGP, and AP. These layers have a yellowish-white tone combined with a rough surface, although the thickness could be different in each vase (Fig. 4a). In terms of element compositions, the CaO contents of the vases show varieties, and trace element patterns generally show different behaviours (Fig. 6). Enrichment of Zn for the white paint is also observed as in the other painted layers for the vases. According to studies on white pigment, it was determined that Ca or Mg clays were used as white pigments in the various local workshops in a wide period (Ferrence et al., 2002; Mastrotheodoros et al., 2013). However, a clear distinction between different workshops could not have been assigned regarding the MgO and CaO contents of white paints (Mastrotheodoros et al., 2013). In this study meantime, vases with white decorations by the same painter were not available for investigation; still, it is important to observe Zn enrichment for the white layers as well.

3.5. Identification of The Painter

Figure 6 represents the trace element patterns of black gloss, dark red, white paint layers, and corresponding body clay pastes of the vases. Paint and body clay pastes show similar patterns, however, different levels of Zn enrichment. Recent theories on the preparation of black gloss suggested selecting a different clay source, particularly for the slip material or using the body clay after the levigation process. Chaviara and Aloupi-Siotis (2016) argued different clay sources were used for the slip material because Zn concentrations and Zn/Ti ratios in black gloss were in accordance with the specific clay sources from five different locations. They also suggested the presence of calamine mineral in the natural clay could transform to $Zn(OH)_2$ during the levigation, and "The natural presence of soluble Zn salts could also account for the significant variation of Zn observed in the ancient samples" (Chaviara and Aloupi-Siotis, 2016). Walton et al. (2015), on the other hand, concluded that similar rare earth element (REE) patterns of black gloss and ceramic body except for Ce anomaly suggested the same origin for the clay of body and black gloss.

The negative correlation of Zn and CaO in the black gloss layers (Fig. 2) may indicate the elevated Zn levels in black gloss were related to the levigation procedure as Walton suggested (2015). On the other hand, the elevated V and Cu levels in the black and red layers, respectively, could indicate either different sources for each paint material or different treatments for the same slip material, including the refinement of the clay and pigment addition to obtaining red, white, and black colors
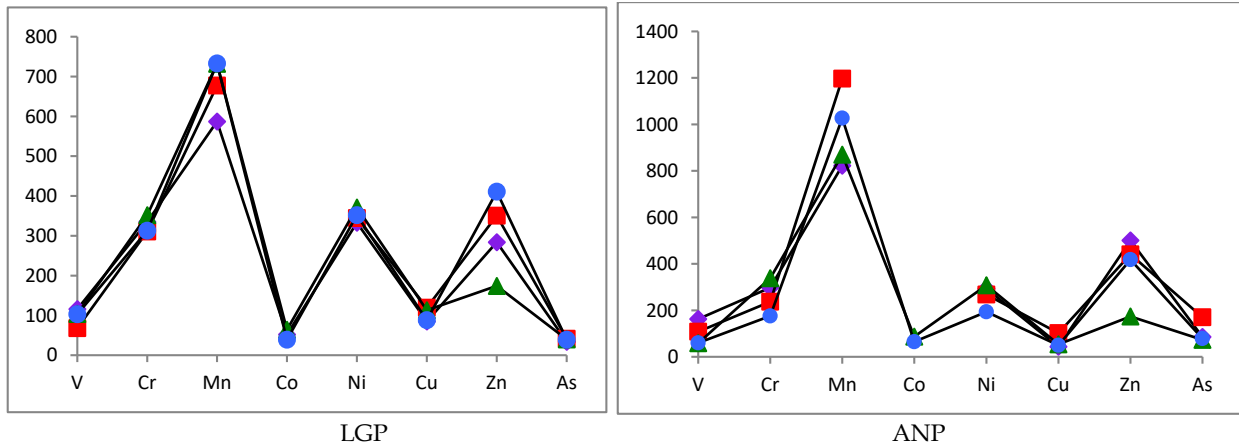
Figure 6. The element patterns of the trace elements (represented as µg.g-1) of the ceramic body and corresponding black gloss dark red and the white paints of each vase (data from Tables 2–5).

The grouping of the dark red paints could be either intentionally by the painter or accidentally, even though the vases worked by the same painter, Sophilos and Lydos, were assigned to the same groups (Fig. 5a). On the other hand, the X-ray penetration to the body clay paste or the black gloss (since the red or white color was applied onto the black gloss) could affect the measurements by interference with the underlying material. To understand if the variables were skewed by the interaction, PCA was used for the data obtained from body and the corresponding dark red and black gloss layers for each vase. In Figure 7, body clay pastes of the vases are distinguished due to their high score in the first component. Meantime, Zn has large negative loadings on the first component. Therefore, black gloss and dark layers are separated from the body clay due to higher values of Zn. The second component has a large positive loading for the Cu (Fig. 7b). Because of this the dark red paint from the black gloss can be recognized by its higher Cu value. Therefore, even though we could not eliminate the possibility of interaction, we conclude that the body and painted layers present a clear distinction that was not dramatically influenced by underlying layers.
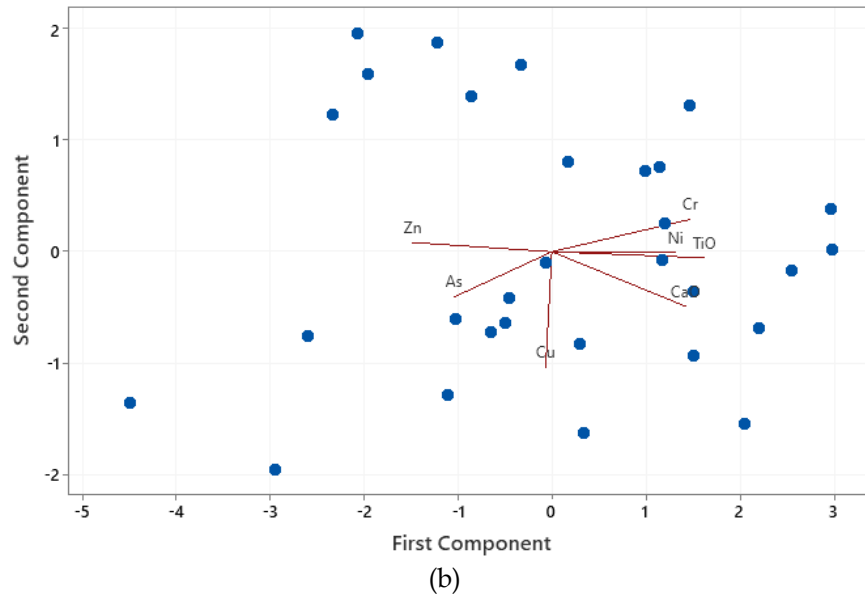

(a)

(b)
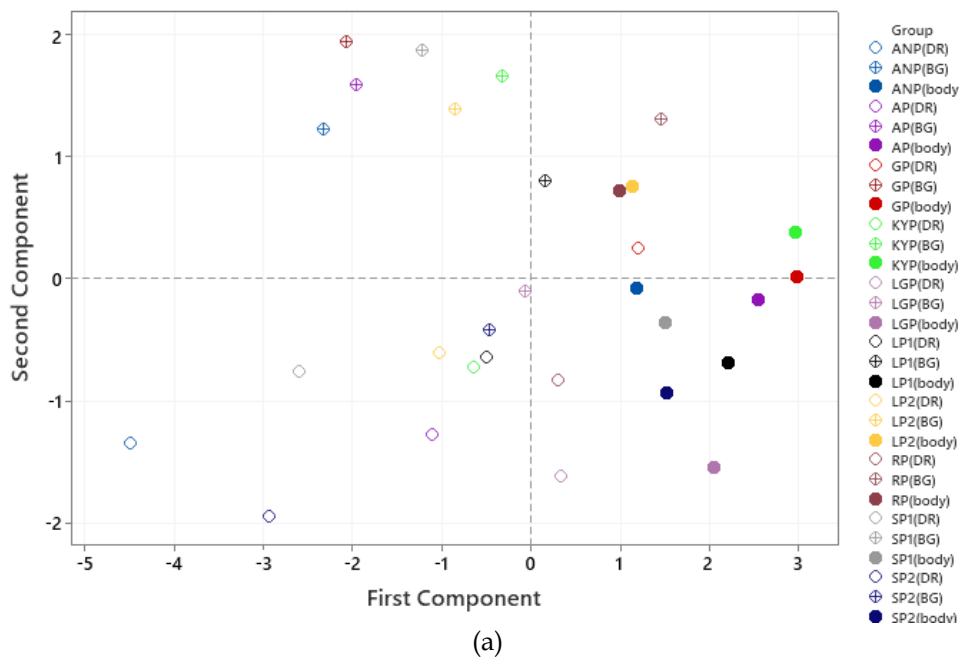
Figure 7. Bivariate plot of PCA using (a) body and corresponding painted layers data of each vase and (b) score and loading principal components 1 and 2.

Since Zn content is emerged to be significant, Zn/Ti ratios of the body, black glosses versus dark layers are plotted to test its efficiency for the characterization of the painter. Fig. 5b presents similar chemical compositional signatures, as the PCA applied for the dark red paint. However, AP and KYP can be recognized as separate vases on the 3D scatterplot. When we consider dark red paint and black gloss together, SP1-SP2 and LP1-LP2 exhibit consistent values, although the vases by Lydos have slightly different ratios for the body (x-axis). The similarity of the vases by Sophilos is significant since there were some disagreements about whether SP1 was a work of Sophilos or his manner (Brownlee, 2013; Bakır, 1981).
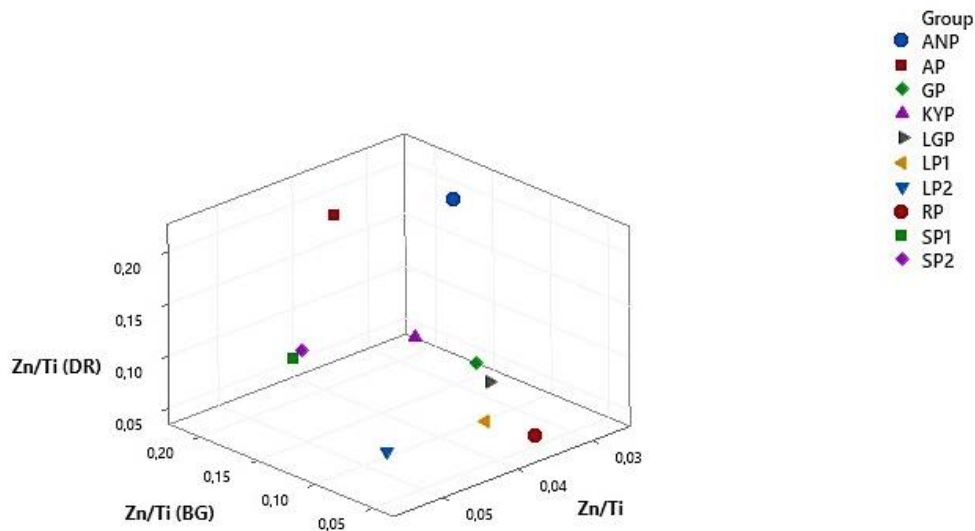

Figure 8. 3D scatter plot of Zn/Ti values in body, black gloss vs. dark red paint.

4. CONCLUSION

The results obtained by the presented study suggest that it may indeed be possible to verify the attribution studies by elemental analysis and identify the characteristics of the vase painters based on the composition of clay mixtures. The elevated Zn levels in each painted layer and the higher V-Cu contents in black gloss and dark red paint may indicate a special treatment to the same clay mixture to achieve the desired color and quality, such as adding pigments and/or refining the clay. The groupings of the vases by the same painters could indicate that the painters were also responsible for the qualification of the pigments as for the paintings. We have established that Zi/Ti ratios could be discriminating features for the painters. It is important since even for the vases attributed to the specific painters, there could be some disagreements between scholars. However, we should investigate other vases by the same painters and include the determination of iron concretions in the black gloss and the dark red layers in further studies.

ACKNOWLEDGEMENTS

REFERENCES

Ali, M.F, Darwish, S.S, and El Sheikha, A.M. (2020) Multispectral analysis and investigation of overlapping layer cartonnage fragments from Egyptian museum, Cairo. *SCIENTIFIC CULTURE,* Vol. 6, No. 3, pp. 25-36. DOI: 10.5281/zenodo.3956805.

Aloupi-Siotis, E. (2008) Recovery and revival of Attic vase-decoration techniques. What can they offer archaeological research? *Lapatin*, pp. 113-128.

Aloupi-Siotis, E. (2020) Ceramic technology: how to characterise black Fe-based glass-ceramic coatings. *Archaeological and Anthropological Sciences*, Vol. 12(8), pp. 1-15.

Aloupi, E., Maniatis, M. (1990) Investigation of the technology of manufacture of local LBA Theran pottery: Body and pigment analysis. *Thera and the Aegean World III*. D. A. Hardy. Thera, Greece, The Thera Foundation, London. 1: pp. 459–469.

Bakır, G. (1981) *Sophilos: ein Beitrag zu seinem Stil* (Vol. 4). P. von Zabern.

Buxeda i Garrigós, J., Cau Ontiveros, M. A. and Kilikoglou, V. (2003) Chemical variability in clays and pottery from a traditional cooking pot production village: testing assumptions in Pereruela. Archaeometry, Vol. 45(1), pp. 1-17.

Boegehold, A.L. (1985). The Time of the Amasis Painter. In D. Bothmer (Ed.), *The Amasis Painter and His World: Vase-Painting in Sixth-Century B.C.* Athens. Malibu: The J. Paul Getty Museum.

Brownlee, A. (2013) Story Line: Observations on Sophilan narrative. In *The ages of Homer: a tribute to Emily Townsend Vermeule,*, J. B. Carter and S. P. Morris (ed.), University of Texas Press.

Cesareo, R., Brunetti, A. and Ridolfi, S. (2008). Pigment layers and precious metal sheets by energy-dispersive x-ray fluorescence analysis. *X-Ray Spectrometry: An International Journal*, Vol. 37(4), pp. 309-316.

Chaviara, A. and Aloupi-Siotis, E. (2016). The story of a soil that became a glaze: chemical and microscopic fingerprints on the Attic vases. *Journal of Archaeological Science: Reports*, Vol. 7, pp. 510-518.

Cohen, B. (1991) The Literate Potter: A Tradition of Incised Signatures on Attic Vases, *Metropolitan Museum Journal*, Vol. 26, pp. 49-95.

Duwe, S. and Neff, H. (2007) Glaze and slip pigment analyses of Pueblo IV period ceramics from east-central Arizona using time of flight-laser ablation-inductively coupled plasma-mass spectrometry (TOF-LA-ICP-MS). *Journal of Archaeological Science*, Vol. 34(3), pp. 403-414.

Ferguson, J. R., Van Keuren, S. and Bender, S. (2015) Rapid qualitative compositional analysis of ceramic paints. *Journal of Archaeological Science: Reports*, Vol. 3, pp. 321-327.

Ferrence, S. C., Betancourt, P. P. and Swann, C. P. (2002) Analysis of Minoan white pigments used on pottery from Kommos, Palaikastro, Mochlos and Knossos. *Nuclear Instruments and Methods in Physics Research Section B: Beam Interactions with Materials and Atoms*, Vol. 189(1-4), pp. 364-368.

Forster, N., Grave, P., Vickery, N., and Kealhofer, L. (2011) Non-destructive analysis using PXRF: methodology and application to archaeological ceramics. *X-Ray Spectrometry*, Vol. 40(5), pp. 389-398.

Gangas, N. H. J., Sigalas, I. and Moukarika, A. (1976). Is the history of an ancient pottery ware correlated with its Mössbauer spectrum?. *Le Journal de Physique Colloques,* Vol. 37(C6), pp. C6-867.

Kingery, W.D. (1991) Attic Pottery Gloss Technology. *Archaeomaterials, Vol.* 5, pp. 47–54.

Liassarrague, F. (1997) Le peintre des demi –palmettes: aspects iconographiques. In *Athenian Potters and Painters,* J. Oakley et al. (ed), Oxbow, Oxford, pp. 125-139.

Liritzis, I., and Zacharias, N. (2011). Portable XRF of archaeological artifacts: current research, potentials and limitations, In *X-Ray Fluorescence Spectrometry (XRF) in Geoarchaeology*. New York, Springer, pp. 109-142.

Liritzis, I., Zacharias, N., Papageorgiou, I., and Tsaroucha, A. (2018). Characterisation and analyses of museum objects using pXRF: An application from the Delphi Museum, Greece. *Studia Antiqua et Archaeologica*, Vol. 24(1), pp. 31-50.

Liritzis, I., Xanthopoulou, V., Palamara, E., Papageorgiou, I., Iliopoulos, I., Zacharias, N. and Karydas, A. G. (2020) Characterization and provenance of ceramic artifacts and local clays from Late Mycenaean Kastrouli (Greece) by means of p-XRF screening and statistical analysis. *Journal of Cultural Heritage*, Vol. 46, pp. 61-81.

Liritzis, I, Laskaris, N, Vafiadou A, Karapanagiotis I, Volonakis, P, Papageorgopoulou, C, Bratitsi, M (2020) Archaeometry: an overview. *SCIENTIFIC CULTURE*, Vol. 6, No. 1, pp. 49-98. DOI: 10.5281/zenodo.3625220.

Lühl, L., Hesse, B., Mantouvalou, I., Wilke, M., Mahlkow, S., Aloupi-Siotis, E. and Kanngiesser, B. (2014) Confocal XANES and the Attic black glaze: the three-stage firing process through modern reproduction. *Anal. Chem.,* Vol. 86 (14) pp. 6924-693.

Maniatis, Y., Aloupi, E. and Stalios, A.D. (1993) New evidence for the nature of the attic black gloss. *Archaeometry, Vol.* 35, pp. 23–24.

Maniatis, Y., Shortland, A. J., Freestone, I. and Rehren, T. (2009) *From Mine to Microscope: Advances in the Study of Ancient Technology*. The Emergence of Ceramic Technology and its Evolution as Revealed with the use of Scientific Techniques. Oxford.

Mastrotheodoros, G., Beltsios, K. G. and Zacharias, N. (2010). Assessment of the production of antiquity pigments through experimental treatment of ochres and other iron-based precursors. *Mediterranean Archaeology and Archaeometry*, Vol. 10(1), pp. 37-59.

Mastrotheodoros, G., Beltsios, K. G., Zacharias, N., Aravantinos, V. and Kalliga, K. (2013) Decorated archaic pottery from the Heracles Sanctuary at Thebes: a materials, technology and provenance study. *Archaeometry*, Vol. 55(5), pp. 806-824.

Mirti, P. Perardi, A., Gulmini, M. and Preacco, M. C. (2006) A scientific investigation on the provenance and technology of a black-figure amphora attributed to the Priam group. *Archaeometry, Vol.* 48.1, pp. 31-43.

Morris, I. (1994). Archaeologies of Greece. In *Classical Greece: Ancient Histories and Modern Archaeologies,* I. Morris (ed.), Cambridge, Cambridge University Press, pp. 8– 47.

Pevnick, S. (2010) Loaded Names, Artistic Identity, and Reading an Athenian Vase, *Classical Antiquity*, Vol. 29, pp. 222-249.

Popelka-Filcoff, R. S., Robertson, J. D., Glascock, M. D. and Descantes, C. (2007) Trace element characterization of ochre from geological sources. *Journal of Radioanalytical and Nuclear Chemistry*, Vol. 272(1), pp. 17-27.

Roux, V. (2020) Roux, V. (2020). Chaîne opératoire, technological networks and sociological interpretations. *Cuadernos de Prehistoria y Arqueología de la Universidad de Granada*. Vol. 30, pp. 15-34.

Shackley, M. S. (2011) X-ray fluorescence spectrometry in twenty-first century archaeology. In *X-Ray Fluorescence Spectrometry (XRF) in Geoarchaeology*. New York, Springer, pp. 1-6.

Shoval, S. and Gilboa, A. (2016) PXRF analysis of pigments in decorations on ceramics in the East Mediterranean: A test-case on Cypro-Geometric and Cypro-Archaic Bichrome ceramics at Tel Dor, Israel. *Journal of Archaeological Science: Reports*, Vol. 7, pp. 472-479.

Tang, C. C., MacLean, E. J., Roberts, M. A., Clarke, D. T., Pantos, E. and Prag, A. J. N. W. (2001) The study of Attic black gloss sherds using synchrotron X-ray diffraction. *Journal of Archaeological Science, Vol.* 28.10, pp. 1015-1024.

Tite, M. S., Bimson, M. and Freestone, I. C. (1982) An examination of the high gloss surface finishes on Greek Attic and Roman Samian wares. *Archaeometry*, Vol. 24(2), pp. 117-126.

Tuna-Nörling, Y. (1995). *Die attisch-schwarzfigurige Keramik und der attische Keramikexport nach Kleinasien: Die Ausgrabungen von Alt-Smyrna und Pitane*. Istanbuler Forschungen.

Turner, M. (2000) Attribution and Iconography. *Mediterranean Archaeology, Vol. 13, pp.* 55-66.

Van Keuren, S., Neff, H. and Agostini, M. R. (2013) Glaze-paints, technological knowledge, and ceramic specialization in the fourteenth-century Pueblo Southwest. *Journal of Anthropological Archaeology*, Vol. 32(4), pp. 675-690.

Walton, M., Trentelman, K., Cianchetta, I., Maish, J., Saunders, D., Foran, B. and Mehta, A. (2015) Zn in Athenian black gloss ceramic slips: a trace element marker for fabrication technology. *Journal of the American Ceramic Society*, Vol. 98(2), pp. 430-436.

Williams-Thorpe, O. (2008) The application of portable X-ray fluorescence analysis to archaeological lithic provenancing. In *Portable X-ray fluorescence spectrometry: capabilities for in situ analysis,* P.J., Potts and M. West (eds), Cambridge, The Royal Society of Chemistry, pp. 174-205.

APPENDIX 1 - CATALOGUE

1. GP

Inventory number: 5811
Dimensions: Height 11 cm, rim diameter: 4 cm, foot diameter: 4 cm
Form: Olpe
Painter: Gorgon

The vase from Çandarlı (Pitane) is on the exhibition in İzmir Archaeology Museum. There is a lion depicted on the front. Characteristic detail of teeth made by incision indicates the work of Gorgon painter. Tuna Nörling attributed the vase to Gorgon painter (1995).

2. SP1

Inventory number: 3332
Dimensions: Height 71 cm.
Form: Lebes Gamikos
Painter: Sophilos

The vase is on the exhibition in İzmir Archaeology Museum. It was found at the excavations in Smyrna. Lebes Gamikos is a term that was created by the combination of the word 'Gamikos', which means marriage, and 'Lebes', and therefore it was defined as a marriage bowl. The vase attributed to Sophilos by Bakır (1981, no. A21).

The body is divided into five friezes.
Body 1: floral, rosettes
Body 2A: The wedding of Helen and Menelaos. Helen is accompanied probably with Meneloas in the first chariot and in the second are Kastor and Polydeukes.
Body 2B: floral, lotus palmette cross between
Body 3: Animal frieze, lion and siren
Body 4: Animal frieze, lion, boar and siren

3. SP2

Inventory number: 9537
Dimensions: Height 30 cm.
Form: Louterion
Painter: Sophilos

The vase form Phokaia is on the exhibition in İzmir Archaeology Museum. Although it is incomplete on the spot side, it appears that this side was decorated with two confronted sphinxes and the other side with confronted a lion and a boar. It was attributed to Sophilos painter by Bakır (1981, no. A19).

4. KYP

Inventory number: 5662
Dimensions: Height 9 cm, rim diameter: 20 cm, foot diameter: 7 cm
Form: Louterion
Painter: KY painter

This kylix is on display in İzmir Archaeology Museum. It was found in Pitane-Çandarlı excavations. The vase was attributed by Tuna Nörling to KY painter (1995).
Decoration A, B: Komos, draped men dancing (3 figures on each side)

5. RP

Inventory number: 13753
Dimensions: Lip diameter: 20 cm
Form: Siana kylix
Painter: Rhodes 12264

This Siana kylix is on display in İzmir Archaeology Museum. It was found in Smyrna excavations. On both sides, the same scene is depicted. This kylix is similar to the works of Rhodos 12264 group (Tuna-Nörling).
Decoration A, B: Chariot race
Tondo: Gorgon head

6. LP1

Inventory number: 8089
Dimensions: 16 cm, width: 15 cm.
Form: Oinochoe
Painter: Lydos (?)

It is on exhibition in İzmir Archaeology Museum. The style of the figures and the scene indicate that the vase is a work of Lydos.
Decoration: Youth, bird, horseman, sitting man

7. LP2

Inventory number: 4889
Dimensions: Height: 17cm, foot diameter: 6 cm
Form: Oinochoe
Painter: Lydos (?)

The oinoche from Çandarlı (Pitane) excavations is on the display in İzmir Archaeology Museum. The style of the figures suggests that the vase is a work of Lydos.
Decoration: Two confronted swans, lotus palmette cross between

8. LGP

Inventory number: 8090
Dimensions: Height: 18 cm
Form: Lekythos
Painter: Leargos Group (?)
The vase is exhibited in İzmir Archeology Museum. The style of the figures and the scene indicate that the vase belongs Leargos Group.
Decoration: Two warriors between onlookers
Shoulder: Siren between two roosters

9. AP

Inventory number: 12456
Dimensions: Height: 44 cm
Form: Amphora
Painter: Affecter (?)

The vase is on the exhibition in İzmir Archeology Museum. One side is incomplete, only lower leg of a warrior is preserved. The style of the figures and the scene indicate that the vase could be attributed to Affecter Painter.
Decoration A: Two warriors, two female on both sides

10. ANP

Inventory number: 16582
Dimensions: Height: 19 cm
Form: Lekythos
Painter: Antimenes (?)

The vase from Gryneion is displayed in İzmir Archeology Museum. The style of the horse and the scene indicate that the vase is a work of Antimenes Painter.
Decoration: Horseman between two warriors and by-siders.